An Adaptive Norm Algorithm for Image Restoration

Daniele Bertaccini[1], Raymond H. Chan[2], Serena Morigi[3], and Fiorella Sgallari[3]

[1] Department of Mathematics, University of Roma "Tor Vergata", Rome, Italy
bertaccini@mat.uniroma2.it
[2] Department of Mathematics, The Chinese University of Hong Kong, Hong Kong, P.R. China
rchan@math.cuhk.edu.hk
[3] Department of Mathematics-CIRAM, University of Bologna, Bologna, Italy
{morigi,sgallari}@dm.unibo.it

Abstract. We propose an adaptive norm strategy designed for the restoration of images contaminated by blur and noise. Standard Tikhonov regularization can give good results with Gaussian noise and smooth images, but can over-smooth the output. On the other hand, L_1-TV (Total Variation) regularization has superior performance with some non-Gaussian noise and controls both the size of jumps and the geometry of the object boundaries in the image but smooth parts of the recovered images can be blocky. According to a coherence map of the image which is obtained by a threshold structure tensor, and can detect smooth regions and edges in the image, we apply L_2-norm or L_1-norm regularization to different parts of the image. The solution of the resulting minimization problem is obtained by a fast algorithm based on the half-quadratic technique recently proposed in [2] for L_1-TV regularization. Some numerical results show the effectiveness of our adaptive norm image restoration strategy.

1 Introduction

The recent increase in the widespread use of digital imaging technologies in consumer (e.g., digital camera and video) and other markets (e.g., medicine imaging) has brought with it a simultaneous demand for image denoising and deblurring.

The most common image degradation model, where the observed data $f \in \mathbb{R}^{n^2}$ are related to the underlying $n \times n$ image rearranged into a vector $u \in \mathbb{R}^{n^2}$, is

$$f = Bu + e, \tag{1}$$

where $e \in \mathbb{R}^{n^2}$ accounts for the perturbations and B is a $n^2 \times n^2$ matrix representing the optical blurring.

The computation of a useful approximation of u can be accomplished by replacing the linear system of equations (1) by a nearby system, whose solution is less sensitive to the noise e. This replacement is commonly referred to as regularization.

A.M. Bruckstein et al. (Eds.): SSVM 2011, LNCS 6667, pp. 194–205, 2012.

The standard Tikhonov regularized solution of the inverse problem for two dimensional image restoration of the observed image f, is the minimum of the functional

$$J(u) = \frac{1}{p}\|Bu - f\|_p^p + \frac{\mu}{q}\|Au\|_q^q, \tag{2}$$

for $p = 2, q = 2$, where A is a regularization operator, and μ is the regularization parameter that controls the trade-off between data fitting term and the regularization term. The use of the Euclidean norm in (2) yields a least squares problem to which many efficient algorithms exist [15,16]. However, the result is only optimal when noise in the image f is white Gaussian noise, (e.g. no outliers) and the solution is smooth, i.e., without discontinuities.

For the regularization term, there has been a growing interest in using the L_1 norm ($q = 1$). The minimization problem (2) with $p = 2, q = 1$, and $A = \nabla$ (the gradient operator), becomes convex but non-smooth and it is denoted by L_2-TV regularization. While a number of algorithms [9,10], have been proposed to solve this optimization problem, it remains a computationally expensive task that can be prohibitively costly for large problems and for operators without a fast implicit implementation or a sparse explicit matrix representation. Recently, the L_1-TV functional, corresponding to the choice $p = 1, q = 1$, $A = \nabla$ in (2) [2,12,13,11], has attracted attention due to a number of advantages, including superior performance with non-Gaussian noise such as impulse noise. The solutions are very stable with respect to outliers and moreover TV controls both the size of jumps and the geometry of the object boundaries in the image.

The main goal of this work is to adaptively consider a suitable norm ($q = 1$ or $q = 2$) according to the determined image structures (smooth regions or edges). Although, the same presented framework can be considered on p, that is on the data fitting term. The L_2-norm regularization well restores corrupted images with wide smooth regions but it oversmoothes the resulting images. On the other hands, the L_1-TV regularization has been successfully applied to restore images because of its good property in preserving edges but in general, the resulting images are blocky. Driven by a suitable map of the structures of the image, we can apply the appropriate norm to selected parts of the image domain.

To achieve this aim, we introduce a measure of the coherence in the image by mean of a threshold structure tensor [8] which provides a coherence map of the image. Following the coherence map we use L_2-norm for pixels in smooth regions and L_1-TV for pixels along edges and corners.

In Fig. 1(a) a simple test image is shown with a white square in a black background corrupted by Gaussian blur and Gaussian noise. The restored image obtained by solving (2) with $p = 2, q = 2$ is shown in Fig. 1(b), The restored images with $p = 1, q = 1$ is shown in Fig. 1(c), while the proposed adaptive approach is shown in Fig. 1(d). Comparing the images in Fig. 1(b),(c),(d) it is clear how an adaptive choice can lead to denoised homogenous regions without blocky effects. In fact it takes advantage of the L_2 approach in the homogeneous regions while keeping the edges thanks to the L_1-TV method.

The paper is organized as follows. We briefly describe the half-quadratic algorithm for L_1-TV image restoration in Section 2. The proposed model and its

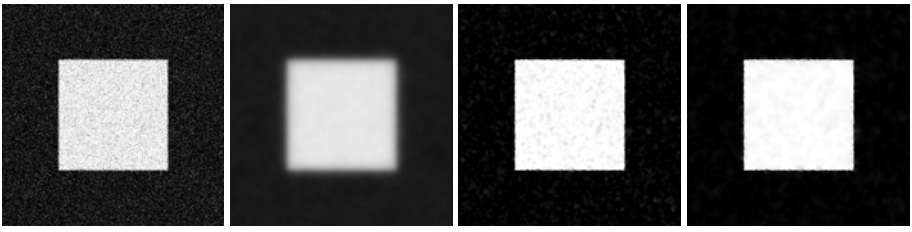

(a) (b) (c) (d)

Fig. 1. (a) corrupted image by white Gaussian noise with `band` = 5, `sigma` = 3 and noise level $\nu = 0.05$; (b) restoration by (2) with $p = 2$, $q = 2$, ($SNR = 9.62$); (c) restoration by L_1-TV (2) with $p = 1$, $q = 1$, ($SNR = 20.30$); (d) restoration by our proposal (adaptive-norm model (11) with $p = 1$), ($SNR = 20.93$), $\mu_1 = 0.5$, $\mu_2 = 90$.

numerical aspects are discussed in Section 3. Numerical examples and comments are provided in Section 4. Section 5 contains concluding remarks.

2 Description of the HQ-Algorithm for L_1-TV Regularization

Let us briefly summarize a recently proposed algorithm [2] that minimizes in a fast and accurate way (2) with $p = q = 1$, that is, with the notation of [2],

$$\min_u \left\{ \sum_{i=1}^{n^2} |B_i\, u - f_i|_\gamma + \mu |\nabla u_i|_\beta \right\}, \tag{3}$$

where B_i is the ith row of the discrete data fidelity operator B; and β and γ are both small positive regularization parameters which prevents the denominator from vanishing in numerical implementations. The specification of β and γ involves trade-offs between the quality of edges restored and the speed in converging. Precisely, the smaller β and γ are, the higher quality of the restoration on the edges will be. We used the notation

$$|\nabla u_i|_\beta = \left((\nabla_x u_i)^2 + (\nabla_y u_i)^2 + \beta \right)^{1/2},$$

$$|B_i u - f_i|_\gamma = \left((B_i u - f_i)^2 + \gamma \right)^{1/2},$$

where ∇_x, ∇_y are the first order finite difference operators in the horizontal and vertical directions, respectively.

The proposed idea is based on an iterative reweighting of a *half-quadratic* algorithm (HQA) for L_1-TV image restoration. Half-quadratic regularization, was introduced in [4,14], and is based on the following expression for the modulus of a real, nonzero number x:

$$|x| = \min_{v>0} \left\{ v\, x^2 \, + \, \frac{1}{4\, v} \right\}, \tag{4}$$

whose minimum is at $v = \frac{1}{2\,|x|}$, and the function in the curly bracket in (4) is quadratic in x but not in v; hence the name *half-quadratic*.

By using (4), the minimum of the function in (3) can be found by applying an alternate minimization procedure to minimize the operator $\mathcal{L}$, i.e.,

$$\min_{u,\, v>0,\, w>0} \mathcal{L}(u, v, w),$$

where

$$\mathcal{L}(u, v, w) = \sum_{i=1}^{n^2} \left[\mu \left(v_i |\nabla u_i|_\beta^2 + \frac{1}{4\, v_i} \right) + w_i |B_i\, u - f_i|_\gamma^2 + \frac{1}{4 w_i} \right] \tag{5}$$

With the notation in [2], we need to perform in sequence the three iterative minimizations, for each iteration step k, that is

$$v^{(k+1)} = \arg\min_{v>0} \mathcal{L}(u^{(k)}, v, w^{(k)}),$$

with explicit solution

$$v_i^{(k+1)} = \left(2 |\nabla u_i^{(k)}|_\beta \right)^{-1} \tag{6}$$

and

$$w^{(k+1)} = \arg\min_{w>0} \mathcal{L}(u^{(k)}, v^{(k+1)}, w),$$

with explicit solution

$$w_i^{(k+1)} = \left(2 |B_i u^{(k)} - f_i|_\gamma \right)^{-1} \tag{7}$$

and

$$u^{(k+1)} = \arg\min_{u} \mathcal{L}(u, v^{(k+1)}, w^{(k+1)}), \tag{8}$$

whose solution u can be found by imposing that:

$$\nabla_u \left(\mathcal{L}(u, v^{(k+1)}, w^{(k+1)}) \right) = 0. \tag{9}$$

This leads to the sequence of linear systems for updating $u^{(k+1)}$:

$$\left[\mu\, A^T\, \widehat{D}_\beta(u^{(k)})\, A + B^T\, D_\gamma(u^{(k)})\, B \right]\, u^{(k+1)} \;=\; B^T\, D_\gamma(u^{(k)})\, f, \tag{10}$$

where $A \in \mathbb{R}^{2n^2 \times n^2}$ is the matrix discretizing the gradient operator $[\nabla_x^T;\ \nabla_y^T]$ with, e.g., first order finite differences (this is the choice in our experiments), $\widehat{D}_\beta(u^{(k)}) := diag(D_\beta(u^{(k)}), D_\beta(u^{(k)}))$, and the weight component matrices $D_\beta(u^{(k)})$, $D_\gamma(u^{(k)})$ are diagonal matrices whose ith entries are given by

$$\left(D_\beta(u^{(k)}) \right)_i = 2 v_i^{(k+1)} = \frac{1}{|\nabla u_i^{(k)}|_\beta},$$

$$\left(D_\gamma(u^{(k)})\right)_i = 2w_i^{(k+1)} = \frac{1}{|B_i\, u^{(k)} - f_i|_\gamma}, i = 1, ..., n^2.$$

In order to get an approximate L_1-TV restoration, given an initial image f and an initial guess for the recovered image $u^{(0)}$, there is just the need to apply an iterative linear solver to (10) like conjugate gradients method for $k = 0, 1, \ldots, k_{\max}$.

We note that other reweighted least squares approachs can be considered such as the one in [6] where an inexact Newton strategy is used to solve the system (10).

3 The Adaptive Norm Algorithm (ANA)

The L_1-TV restoration algorithm HQA, developed by [2] and summarized in Section 2, works very well especially in presence of salt-and-pepper noise and near edges and corners. On the other hand, with different types of image perturbations, like the white Gaussian noise, and in the presence of smooth, homogeneous regions and weak edges it can provide a less accurate restoration and can give artifacts like, e.g., a blocky effect in smooth regions. A *selective reweighted of the half-quadratic approach* is one of the possible natural ways to overcome these well-known issues of the L_1-TV restoration. With the word *selective* we mean "using different norm for different pixels" of the image. To achieve this aim, one could work with a norm continuously changing from 1 to 2, but this would lead to the solution of a PDE derived from the variational problem similar to (2). A preliminary step in this direction has been proposed by [18]. In contrast, we choose not to change the norm continuously from 1 to 2, but, using a suitable *coherence map*, we classify the pixels in the image as pixels belonging to homogeneous region or pixels belonging to edges or corners, and we associate them with norm L_2 or L_1, respectively. Details on the construction of the coherence map C are given in Section 3.1.

Driven by the coherence map, we use the L_2 norm for smooth and homogeneous regions and the L_1 norm near edges and corners. Let C be a diagonal matrix with the ith entry $(C)_i = 1$ if the ith pixel belongs to a homogeneous region identified by the coherence map, while $(C)_i = 0$ near edges. Let $\bar{C} = I - C$, with I the identity matrix. In view of this, we propose to modify the functional in (2) to the following functional

$$\Phi(u) = \|Bu - f\|_1^1 + \mu_1 \|CAu\|_1^1 + \mu_2 \|\bar{C}Lu\|_2^2, \tag{11}$$

where μ_1, μ_2 are regularization parameters, L is a regularization operator, such as for example $L = A$ or, e.g., the discrete Laplacian, and A is defined as in (10). This new functional also caters for different regularization operators. Moreover, the adaptive norm strategy can also be applied to the data fidelity term $Bu - f$ in (11).

The minimization of the functional (11) can be obtained in a way similar to what is done for the half quadratic L_1-TV and, in particular, by solving the following linear systems for updating $u^{(k+1)}$

$$\left[(\mu_1 A^T C \widehat{D}_\beta(u^{(k)}) CA + \mu_2 L^T \bar{C} L + B^T D_\gamma(u^{(k)}) B\right] u^{(k+1)} = \\ = B^T D_\gamma(u^{(k)}) f \tag{12}$$

where the weight component matrix $\widehat{D}_\beta(u^{(k)})$, incorporates the selective L_1/L_2 reweighted by the diagonal matrix C. We initialized the iterative process by setting $u^{(0)} = f$, and the coherence map is computed at each iteration step k. In the following we will name our algorithm Adaptive Norm Algorithm (ANA).

In order to accelerate the solution of (12) the strategy used for sequences of linear systems proposed in [1] can be used. However we found that stopping the conjugate gradient solver after a few iterations already gives good results; see Section 4 for numerical examples.

The model (11) allows the use of the techniques in [2] to prove the convergence of sequence $\{u^{(k)}\}$ to a minimum of $\Phi(u)$. An analysis of the convergence of the sequence $\{u^{(k)}\}$ generated by the proposed adaptive norm strategy can be based on the analysis of the convergence of half-quadratic algorithm in [2].

3.1 The Coherence Matrix Construction

In order to detect if a pixel of the given image belongs to an edge or a homogeneous region, we need a strategy that is able to mark each pixel with a score that we normalize in the range $[0, 1]$.

Coherence enhancing image smoothing has been introduced in [8] and successfully applied in image filtering by anisotropic diffusion. This type of nonlinear diffusion includes the construction of a diffusion tensor which is built as follows. Given an image u, and its Gaussian-smoothed version u_σ, a regularized shape descriptor is provided by

$$S_\delta(\nabla u_\sigma) := (K_\delta * (\nabla u_\sigma \otimes \nabla u_\sigma)) \tag{13}$$

where K_δ is a Gaussian kernel with $\delta \geq 0$. The matrix S_δ is symmetric positive semi-definite and its eigenvalues $\lambda_1 \geq \lambda_2$ integrate the variation of the gray values within a neighborhood of size $O(\delta)$. They describe the average contrast in the corresponding eigendirections $\mathbf{v}_1$ and $\mathbf{v}_2$. The orientation of the eigenvector $\mathbf{v}_2$, corresponding to the smaller eigenvalue, represents the direction of lowest fluctuations, the so-called coherence orientation. In this way, constant areas are characterized by $\lambda_1 = \lambda_2 = 0$, while straight edges give $\lambda_1 \gg \lambda_2 = 0$.

The normalized coherence value which measures the anisotropic structures within a window of scale δ is thus defined as

$$c = \frac{(\lambda_1 - \lambda_2)^2}{\max\{(\lambda_1 - \lambda_2)^2\}}, \quad c \in [0, 1]. \tag{14}$$

Thus, for anisotropic structures, c approaches 1, while it tends to zero for isotropic structures. Let c_i be the coherence value obtained by computing (14) for the ith pixel in the vectorized image u. We use a "selective" threshold parameter τ (typically $0 \ll \tau < 1$) to construct the diagonal matrix C, with $(C)_i = 1$

when the ith pixel belongs to a homogeneous region, that is when $c_i < \tau$, while $(C)_i = 0$ near edges. This aim to partition the image into homogeneous and non-homogeneous regions, different partitioning will be further investigated.

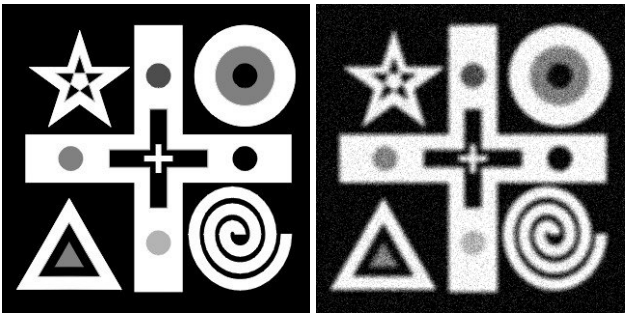

(a) (b)

Fig. 2. Example 1:(a) Blur- and noise-free 320×320 image; (b) corrupted image by symmetric Gaussian blur with `band` $= 7$ and `sigma` $= 5$, noise level $\nu = 0.02$

4 Experiments and Results

Let $u \in \mathbb{R}^{n^2}$ represent a blur- and noise-free image. We generate an associated blurred and noise-free image $\hat{f}$ by multiplying u by a block Toeplitz matrix $B \in \mathbb{R}^{n^2 \times n^2}$ with Toeplitz blocks. The matrix B represents a symmetric Gaussian blurring operator and has two parameters `band` and `sigma`. The former specifies the half-bandwidth of the Toeplitz blocks and the latter the variance of the Gaussian point spread function. The larger the `sigma` is, the more the blurring will be. A blur- and noise-contaminated image $f \in \mathbb{R}^{n^2}$ is obtained by adding an error vector $e \in \mathbb{R}^{n^2}$ to $\hat{f}$.

Thus,

$$f = Bu + e.$$

The corrupted image $f \in \mathbb{R}^{n^2}$ is assumed to be available and we would like to determine the blur- and noise-free image u. In our experiments, e has normally distributed entries with mean zero, scaled to yield a desired noise-level

$$\nu = \frac{\|e\|}{\|u\|}.$$

In all the examples we take the parameters $\beta = 10^{-3}$ and $\gamma = 10^{-6}$ in (3) and we consider periodic boundary conditions for the difference matrix A. Equation (12) is solved by the conjugate gradient method where we stopped when the Euclidean norm of the relative error between successive approximations is less than $5 \cdot 10^{-5}$. The solver is very fast and we do not need to accelerate the solution of (12) by preconditioning strategies.

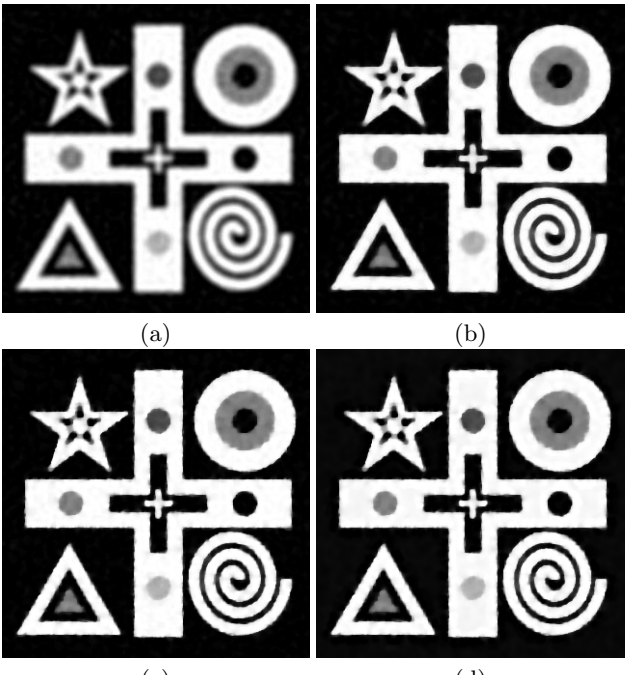

Fig. 3. Example 1: (a) restoration by (2) with $p = 1$, $q = 2$, $\mu = 10$ ($SNR = 10.68$); (b) restoration by L_1-TV (2) with $p = 1$, $q = 1$, $\mu = 0.5$ ($SNR = 15.72$) (c) restoration by ANA with $p = 1$, $\mu_1 = 0.2$, $\mu_2 = 10$ ($SNR = 16.76$); (d) restoration by ANA with adaptivity also for the fidelity term, $\mu_1 = 0.2$, $\mu_2 = 10$ ($SNR = 16.47$)

The displayed restored images provide a qualitative comparison of the performance of the proposed adaptive norm algorithm. A quantitative comparison is given by the Signal-to-Noise Ratio (SNR),

$$\text{SNR} := 10 \log_{10} \frac{\|u - E(u)\|_2^2}{\|\hat{u} - u\|_2^2} \,\text{dB}, \tag{15}$$

where u denotes the blur- and noise-free image, $\hat{u}$ the restored image and $E(u)$ is the mean grey-level value of the original image.

The choice of the parameters μ_1 and μ_2 in (11) clearly affect the quality of the restored image, in our experimentation we have empirically chosen μ_1 in the range $[0, 1]$, and μ_2 in the range $[10, 100]$, but further investigations will be planned. In the literature there are several regularization parameter selection methods for Tikhonov regularization problems ($p = 2, q = 2$), e.g. the discrepancy principle, the L-curve and the Generalized Cross-Validation (GCV) methods [7]. Recently in [17] a generalization of GCV for the case $p = 2, q = 1$ has been proposed.

Table 1. Example 2: Results for restorations of image corrupted by Gaussian blur corresponding to different `band`,`sigma` values, and noise-levels ν. $\mu_1 = 0.2$, $\mu_2 = 5$ (first 8 rows) $\mu_1 = 0.5$, $\mu_2 = 10$ (last 4 rows).

band	sigma	ν	SNR(L_1-TV)	SNR(ANA)
7	5	0.01	22.09	22.90
7	5	0.02	20.08	20.95
7	5	0.05	16.74	17.61
7	5	0.1	13.69	15.20
5	3	0.01	23.63	24.53
5	3	0.02	21.07	22.16
5	3	0.05	18.02	18.76
5	3	0.1	15.10	15.68
3	1	0.01	26.35	26.78
3	1	0.02	23.20	23.98
3	1	0.05	18.69	19.38
3	1	0.1	14.62	15.35

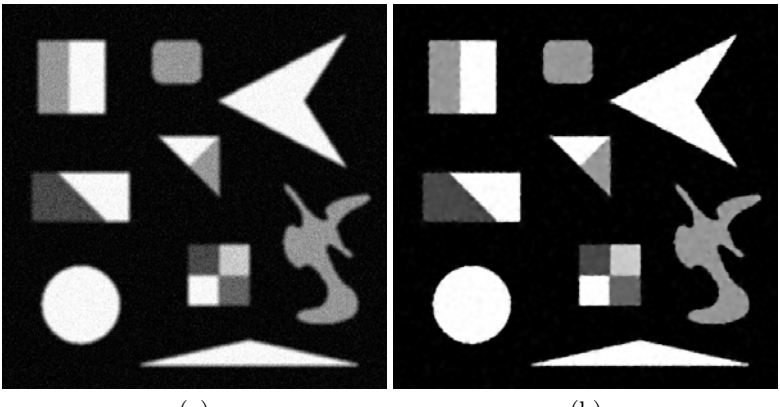

(a) (b)

Fig. 4. Example 2: (a) corrupted 512×512 image by symmetric Gaussian blur with `band` $= 7$ and `sigma` $= 5$, noise level $\nu = 0.02$; (b) restoration by ANA with $p = 1$, $\mu_1 = 0.2$, $\mu_2 = 1$ ($SNR = 20.95$).

Example 1. In this example the image in Fig. 2(a) is corrupted by Gaussian noise, characterized by noise level $\nu = 0.02$, and symmetric Gaussian blur with `band` $= 7$ and `sigma` $= 5$. The corrupted image is shown in Fig. 2(b). The restorations obtained by applying the three approaches (L_2-TV, L_1-TV, ANA) are shown in Figure 3. In Fig. 3 (d) the reconstructed image is obtained by solving (11) with the adaptivity also in the fidelity term. In all the algorithms we have considered $k_{max} = 40$ outer steps in (12) but also less outer steps give satisfactory results. Our ANA gives the best $SNR = 16.76$. From a visual inspection of Fig. 3(c),(d), we observe that $white - homogemous$ regions are clearly better restored.

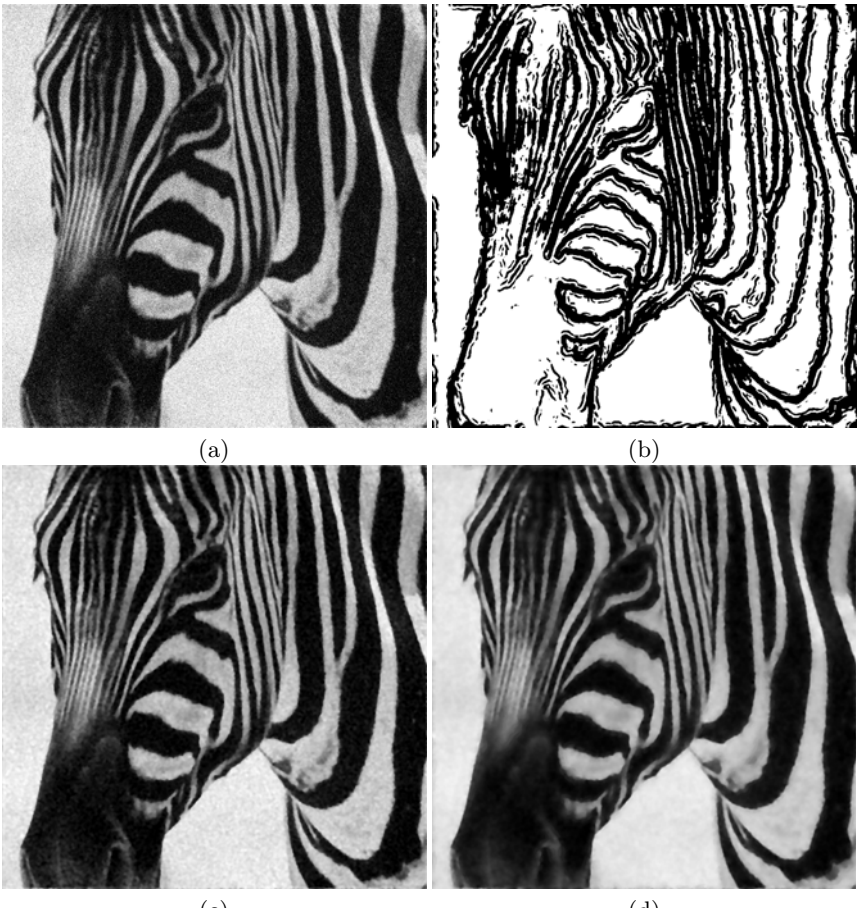

Fig. 5. Example 3: (a) corrupted image ($SNR = 9.43$); (b) coherence map; (c) restoration by L_1-TV (2) with $p = 1$, $q = 1$, $\mu = 0.5$ ($SNR = 17.15$) (d) restoration by ANA with $p = 1$, $\mu_1 = 0.5$, $\mu_2 = 80$ ($SNR = 17.47$)

Example 2. In this example a 512×512 image is contaminated by different noise levels and incremental Gaussian blur. In Fig. 4(a) the corrupted image by Gaussian noise, characterized by noise level $\nu = 0.02$, and symmetric Gaussian blur with `band` $= 7$ and `sigma` $= 5$ is shown, while Fig. 4(b) shows the image restored by ANA using $k_{max} = 30$ outer steps. In Table 1, algorithms L_1-TV and ANA are compared and their SNR values are reported in the fourth and fifth columns, respectively. Table 1 and other additional numerical experiments, indicate that the performance of our method is better for images with quite large homogenous regions, for medium blur and for quite high noise levels.

Example 3. In this example we test our approach on a photographic image of size 800×800 corrupted by symmetric Gaussian blur with `band` $= 5$ and `sigma` $= 3$ and noise level $\nu = 0.02$, shown in Fig. 5(a). The results of applying $k_{max} = 10$ outer steps in (12) are shown in Fig. 5(c), (d) for algorithm L_1-TV and ANA, respectively. We can appreciate the good quality results we get with just a few steps, that demonstrate the efficiency of the algorithm. In Fig. 5(b) the used coherence map is illustrated.

5 Conclusions

In this paper we propose a fast algorithm that allow L_1 or L_2-norm regularization for different image areas according to the image structures (e.g., smooth regions or edges). Numerical experiments seem to confirm that our algorithm is promising. We plan to extend this framework to general L_1-regularized problems and to consider other choices for p and q in model (2).

Acknowledgments. This work has been partially supported by MIUR-Prin 2008, *ex*60% project by University of Bologna "Funds for selected research topics" and by GNCS-INDAM.

References

1. Bertaccini, D., Sgallari, F.: Updating preconditioners for nonlinear deblurring and denoising image restoration. Applied Numerical Mathematics 60, 994–1006 (2010)
2. Chan, R.H., Liang, H.X.: A fast and efficient half-quadratic algorithm for TV-L1 Image restoration, CHKU research report 370 (submitted, 2010), `ftp://ftp.math.cuhk.edu.hk/report/2010-03.ps.Z`
3. Chan, T., Mulet, P.: On the convergence of the lagged diffusivity fixed point method in total variation image restoration. SIAM J. Numer. Anal. 36, 354–367 (1999)
4. Geman, D., Yang, C.: Nonlinear image recovery with half-quadratic regularization and FFTs. IEEE Trans. Image Proc. 4, 932–946 (1995)
5. Jacobson, M., Fessler, J.: An expanded theoretical treatment of iteration-dependent majorize-minimize algorithms. IEEE Trans. Image Proc. 16, 2411–2422 (2007)
6. Rodriguez, P., Wohlberg, B.: Efficient minimization method for a generalized total variation functional. IEEE Transactions on Image Processing 18, 322–332 (2009)
7. Hansen, P.: Rank-Deficient and Discrete Ill-Posed Problems. SIAM, Philadelphia (1998)

8. Weickert, J., Scharr, H.: A scheme for coherence enhancing diffusion filtering with optimized rotation invariance. J. of Visual Communication and Image Representation 13, 103–118 (2002)
9. Vogel, C., Oman, M.: Iterative methods for total variation denoising. SIAM J. Sci. Comp. 17(1-4), 227–238 (1996)
10. Chambolle, A.: An algorithm for total variation minimization and applications. J. of Math. Imaging and Vision 20, 89–97 (2004)
11. Nikolova, M.: A variational approach to remove outliers and impulse noise. J. of Math. Imaging and Vision 20, 99–120 (2004)
12. Nikolova, M.: Minimizers of cost-functions involving nonsmooth datafidelity terms application to the processing of outliers. SIAM J. Numerical Analysis 40, 965–994 (2002)
13. Chan, T.F., Esedoglu, S.: Aspects of total variation regularized L1 function approximation. SIAM J. Appl. Math. 65, 1817–1837 (2005)
14. Nikolova, M., Chan, R.: The equivalence of half-quadratic minimization and the gradient linearization iteration. IEEE Trans. Image Proc. 16, 1623–1627 (2007)
15. Reichel, L., Sgallari, F., Ye, Q.: Tikhonov regularization based on generalized Krylov subspace methods. Appl. Numer. Math. (2010), doi:10.1016/j.apnum.2010.10.002
16. Morigi, S., Reichel, L., Sgallari, F.: An interior-point method for large constrained discrete ill-posed problems. J. Comput. Appl. Math. 233, 1288–1297 (2010)
17. Liao, H., Li, F., Ng, M.: On Selection of Regularization Parameter in Total Variation Image Restoration. Journal of the Optical Society of America A 26, 2311–2320 (2009)
18. Chen, Q., Montesinos, P., Sun, Q.S., Heng, P.A., Xia, D.S.: Adaptive total variation denoising based on difference curvature. Image and Vision Computing 28(3), 298–306